TECHNICAL PAPER

CrossMark

Study of machinability and parametric optimization of end milling on aluminium hybrid composites using multi-objective genetic algorithm

B. Rajeswari[1] · K. S. Amirthagadeswaran[2]

Abstract

Metal matrix composites offer a substantial surety to meet the present and future demands spanning from automobiles to aerospace. Hybrid metal matrix composites are a new choice of materials involving several advantages over the single reinforcement. In this present study, three specimens possessing aluminium 7075 reinforced with particulates of silicon carbide (5, 10, 15% weight percentage) and alumina (5% weight percentage) were developed using stir casting. The purpose of the study was to investigate the effect of reinforcement particles of silicon carbide on the machinability of hybrid metal matrix composites. These materials are engineered to match the requirements of optimal output responses such as low surface roughness, less tool wear, a less cutting force with the high rate of material removal under a set of practical machining constraints. Multi-objective parametric optimization using genetic algorithm obtained optimal cutting responses. The spindle speed, feed rate, depth of cut and weight percentages of SiC were selected as the influencing parameters for meeting the output responses in end milling operation. Based on the Box–Behnken design in response surface methodology, 27 experimental runs were conducted and nonlinear regression models were developed to predict the objective function. The adequacy of the model was checked through ANOVA and was found to be significant. The optimum settings of the parameters were found using multi-objective genetic algorithm. The predicted optimal settings were verified through confirmatory experiments, and the results validated.

Keywords Composites · End milling · Genetic algorithm · Interaction effects · Multi-objective

List of symbols

Ra	Surface roughness (μm)
MRR	Material removal rate (mm³/min)
T_w	Tool wear (mm)
F_z	Cutting force (N)
N	Spindle speed (rpm)
f	Feed rate (mm/rev)
d	Depth of cut (mm)
w	Weight percentage of silicon carbide
DF	Degree of freedom
CI	Confidence interval
VIF	Variance inflation factor

✉ B. Rajeswari
   rajeswari_b@gct.ac.in

1   Department of Mechanical Engineering, Government College of Technology, Coimbatore, Tamil Nadu, India

2   Principal, United Institute of Technology, Coimbatore, Tamil Nadu, India

1 Introduction

Composites are the result of the research in material science with a view of finding potential light weight replacements for heavier materials. Metal matrix composites can be tailored to have superior properties such as high specific strength, stiffness, wear resistance, high-temperature performance, better thermal and mechanical properties, fatigue and creep resistance than those of monolithic alloys. Hybrid particulate-reinforced aluminium composites find diverse applications in automotive, aircraft and locomotive industries due to their increased hardness and strength. Machining is unavoidable in manufacturing, but the machinability of composites is not as that of the matrix material and is hindered by the hardness of the

reinforcements. Hence, machinability studies have acquired greater importance in the area of composites [1–3]. End milling is the widely used operation for metal removal in a variety of manufacturing industries including the automobile and aerospace sector where quality is an important factor in the production of slots, pockets and moulds/dies [4–10]. Hence, more insight into the process is required. A manufacturing industry always aims at producing a large number of products with desired quality at the right time with less cost. This invites the use of multi-objective optimization [11]. There are several multi-objective optimization techniques for the same like goal programming, simulated annealing (SA), grey relational analysis (GRA) and genetic algorithms (GA). The genetic algorithm works with a random population of solution points, and a set of Pareto-optimal solutions is obtained for the best performance measures.

A detailed survey of the research works recently published in journals was studied in depth to acquire knowledge and constraints of the study. Evolutionary algorithms are widely used as they are reasonably accurate [12]. Indrajit et al. [13] reviewed the various evolutionary algorithms used in metal cutting processes. Jawahir et al. [14] consolidated in his studies on the effect of surface integrity and directed that the major challenges in surface integrity studies for the future include the generation and use of new and advanced experimental tools and techniques for comprehensive evaluation of surface integrity from material removal processes. Doriana et al. [15] suggested that the application of the genetic algorithm-based approach in complex machining systems. He concluded that intelligent manufacturing achieves substantial savings in terms of money and time if it integrates an efficient automated process planning module with other automated systems such as production, transportation and assembly.

Senthilkumar et al. [16] obtained a non-dominated solution set to maximize metal removal rate and to minimize surface roughness using genetic algorithm. Vijay Kumar et al. [17] concluded that the experimental values and the regression model values follow an identical trend showing that the models developed are best suited for turning operation. Majumder [18] illustrated the use of three algorithms—particle swarm optimization, simulated annealing and genetic algorithm for optimizing the electric discharge machining process parameters. Hesam et al. [19] investigated the use of micro-genetic algorithm for obtaining good surface finish in EDM process. Thangarasu et al. [20] studied that the major parameters affecting machining quality include surface roughness and material removal rate in AISI 304 stainless steel using MOGA. Ganesan et al. [21] remarked the advantages of multi-objective optimization approach over the single-objective one and highlighted that by means of Pareto-graph several different situations may be considered, facilitating the choice of right parameters for any condition.

Mahfouf et al. [22] compared the GA-based single-objective and the multi-objective optimization algorithms to obtain the optimal combination of the composites and the tempering temperature for optimal design of alloy steels. The results show that the evolutionary multi-objective algorithm (EMO) techniques can be effectively used to deal the optimization problems.

Yadav et al. [23] studied the process parameters of wheel speed, pulse current, pulse on-time and duty factor in electrical discharge diamond face grinding and optimized the material removal rate (MRR) and average surface roughness (Ra) using multi-objective genetic algorithm.

Santhanakrishnan et al. [24] focused on the effect of geometrical and machining parameters such as rake angle, nose radius, cutting speed, feed rate and depth of cut on temperature rise during end milling operation on Al 6351 with high-speed steel end mill cutter using genetic algorithm.

Malghan et al. [25] investigated the multi-objective optimization using the application of particle swarm optimization and response surface methodology for face milling parameters on aluminium matrix composites. They concluded that spindle speed has major contribution followed by feed rate and depth of cut on cutting force, surface roughness and power consumption.

Prabhu et al. [26] studied the optimization of electric discharge machining parameters using fuzzy logic with central composite design of response surface methodology.

The literature survey made shows that limited research has been reported with the application of response surface methodology (RSM)-based genetic algorithm (GA) to optimize the material removal rate, surface roughness, tool wear and cutting force simultaneously.

Most of the studies during machining of Al-based composites reinforced with SiC particles revealed the wear characteristics of tool based on only the effects of cutting parameters like cutting speed, feed rate, depth of cut. The effect of weight percentage of SiC and Al_2O_3 particles has not been examined simultaneously for various machinability characteristics like surface finish, material removal rate, cutting force and tool wear. The formation of continuous chips while machining of aluminium is a serious issue which causes heat generation leading to excess tool wear.

To the authors' best knowledge, no work published evaluates the optimality and the effects of cutting parameters on multi-performance characteristics in end milling process by using RSM and multi-objective genetic algorithm (MOGA). The setting of parameters was accomplished by Box–Behnken design method. The purpose of the present work aims to: i) develop a mathematical model

using spindle speed, feed rate, depth of cut and varying weight percentage of SiC by multiple nonlinear regression for obtaining optimal responses using RSM; ii) obtain Pareto-optimal solutions to acquire appropriate optimal input variables for improving machinability; (iii) investigate the effect of SiC on machinability characteristics of prepared hybrid composites; and iv) study of effect of process parameter on formation of chips during machining.

2 Materials and methods

2.1 Material selection

Aluminium 7075 is used as the base material. Also called aircraft aluminium, Al7075 is widely employed in transport applications, including marine, automotive and aviation, due to their high strength-to-density ratio. Corrosion protection is ensured also in outdoor atmosphere. The reinforcements chosen are silicon carbide and alumina. Owing to their increased hardness and strength, the mechanical properties of the composite are enhanced. The silicon carbide particles size used is 220 meshes, and the average size of alumina used is 45 μm. The density of Al_2O_3 particles is higher than SiC. The alumina particles prevent the oxidation of liquid aluminium. The volume fraction of alumina is kept fixed as 5%. The literature survey suggests that the addition of SiC to 15% increases the mechanical properties of the composite. It is also obvious that the volume fraction of the reinforcement phase as well the matrix properties affects the machinability of the composite. So the three combinations of composites as $90Al7075/5SiC/5Al_2O_3$, $85Al7075/10SiC/5Al_2O_3$ and $80Al7075/15SiC/5Al_2O_3$ were fabricated with the size of 130 mm × 100 mm × 50 mm.

2.2 Stir casting

Stir casting technique is used to fabricate aluminium alloy with varying percentages of silicon carbide and alumina reinforcements. In order to achieve good bonding between the matrix and particulates, one weight per cent of magnesium was added. The stir casting furnace (Fig. 1) is mounted on the floor, and the temperature of the furnace is precisely measured and controlled in order to achieve sound quality composite. The melt was maintained at a temperature between 750 °C and 800 °C for 1 h. Vortex was created by using a mechanical stirrer.

Weighed quantities of SiC and alumina are preheated to 600 °C and added to the melt with constant stirring for about 10 min at 500–650 rpm. After complete addition of the particles to the melt, the composite alloy was tilt-

Fig. 1 Stir casting furnace make: SWAM EQUIP

poured into the preheated (300 °C) permanent steel mould and allowed to cool in atmospheric air. The billet was then removed from the mould and machined to required dimensions.

The microstructures of $Al7075/5\%Al_2O_3/5\%SiC$, $Al7075/5\%Al_2O_3/10\%SiC$ and $Al7075/5\%Al_2O_3/15\%SiC$ are shown in Fig. 2a–c.

In this work L27, orthogonal array of Box–Behnken design of the experiment is used for conducting the end milling operation trials. These three-level estimates provided a simple, efficient and systematic approach to optimizing the design, performance, quality and cost compared to central composite design (CCD). A number of factors such as spindle speed, feed, depth of cut, tool geometry, work/tool materials and cutting conditions affect the machinability characteristics. Four controlling factors, namely spindle speed, feed, depth of cut and weight percentage of SiC, were chosen. These factors were selected from literature study of machining optimization problems and machinability studies [3, 23, 24]. Table 1 lists the machining parameters used as control factors and their levels. The values were taken based on machining settings normally followed in industries for Al7075 with carbide-coated inserts. The range of cutting parameters normally used in the industry for such processes has been adopted.

With a higher proportion of SiC, composite becomes brittle leading to poor surface finish. The combination of cutting parameters coupled with variation in the composition of reinforcement may lead to better performances. Considering these, proportions of SiC was also taken as a factor influencing the machining performance. Machinability was referred by surface finish, tool life, power

Fig. 2 Microstructures of Al7075 composite with alumina 5% and SiC **a** 5%, **b** 10% and **c** 15%
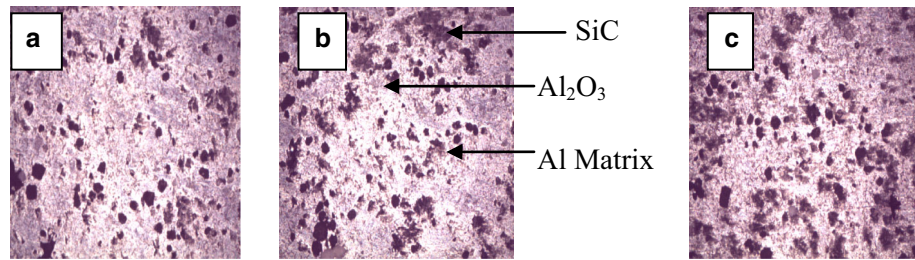
Table 1 Control factors and levels for end milling

Control factors	Levels		
	− 1	0	+ 1
Spindle speed (N) in rpm	1000	1500	2000
Feed rate (f) in mm/rev	0.02	0.03	0.04
Depth of cut (d) in mm	1	1.5	2
Weight percentage of SiC (w)	5	10	15

consumption and material removal rate. So the multi-responses were chosen as surface roughness, MRR, cutting force and tool wear.

2.3 End milling operation

Based on the design matrix, the fabricated composites were end-milled in a BFW Universal Milling Machine (Fig. 3). AXMT 0903 PER-EML TT8020 of Taegu Tec carbide-coated which has helical higher positive cutting edge inserts was used for end milling. Length and diameter of the tool holder are 170 mm and 20 mm, respectively (specification TE90AX 220-09-L). Surface roughness (Ra) was measured using MITUTOYO SJ210 surface tester. Tool flank wear (T_w) was measured using METZER profile projector (model

Fig. 3 BFW universal milling machine

Metz-401). Cutting force (F_z) was measured in Kistler multi-component dynamometer (model 9257B).

Material removal rate (MRR) was calculated as per Eq. (1)

$$\text{MRR} = L * W * D/T \ \left(\text{mm}^3/\text{min}\right) \tag{1}$$

where L—length of specimen (mm), W—width of cut (mm), D—depth of cut (mm), T—time taken for material removal in minutes. Measurements of responses are shown in Fig. 4 (Table 2).

Table 2 shows the experimental parameter settings and the corresponding values of the responses. With the data available in the table, regression models for all the responses were formulated. The details of the models are discussed in the next section.

3 Results and discussion

3.1 Mathematical modelling and optimization

In most of the surface model problems, the form of association between the output and the independent variable is unpredictable. Thus, the first step in RSM is to find a suitable approximation for the true functional relationship between Y and set of independent variables used. Usually, a second-order model is developed in RSM. It is assumed that all the parameters are controllable by experiments with negligible errors. Therefore, a second-order polynomial Eq. (2) can be used to find a suitable functional relationship between the process parameters and the response surface.

$$Y = \beta_0 + \sum_{j=1}^{k} \beta_j X_j + \sum_{j=1}^{k} \beta_{jj} X_j^2 + \sum_{i<}\sum_{j=2}^{k} \beta_{jj} X_i X_j + e \tag{2}$$

where X_j denotes parameters, k is the number of parameters, β_j is the coefficients, e is the random error, and coefficients used in the above model can be calculated by means of using a least squares technique. The second-order model is normally used when the response function is not known or nonlinear. ANOVA was taken into account to estimate the suitability of the regression model. To this end, the ratio of variance due to the effect of the model factors and variance resulting from the error terms, F ratio,
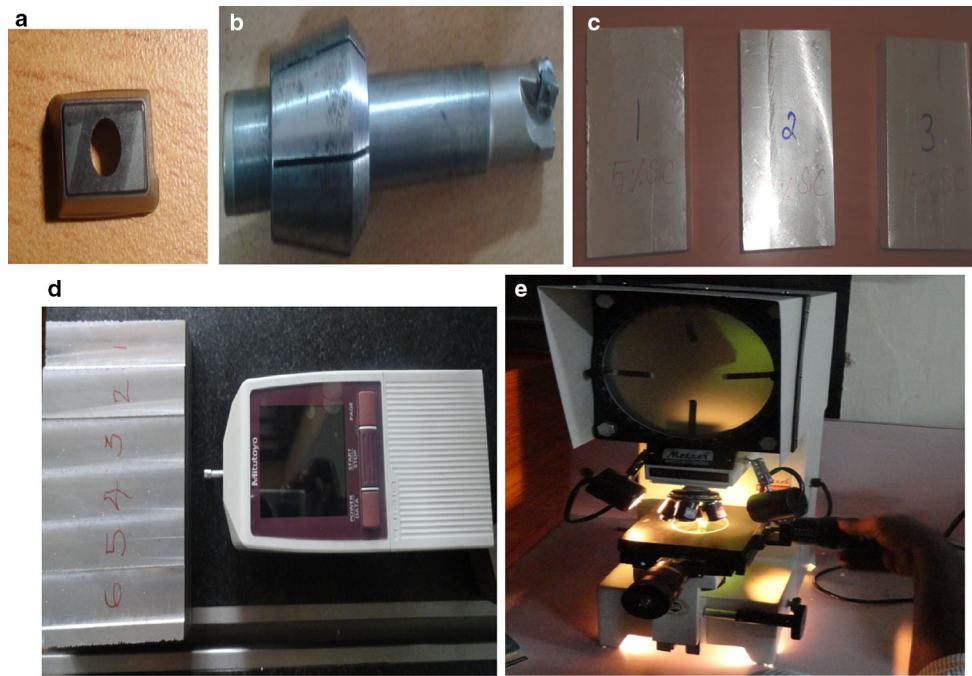
Fig. 4 Measurements of responses. **a** Cutting tool insert, **b** tool holder (TE90AX 220-09-L), **c** workpieces, **d** surface roughness measurement, **e** tool flank wear measurement

was calculated as an ANOVA procedure. F ratio or variance ratio is employed to determine the significance of the model regarding variance of all the terms at an appropriate level of a. The aim of RSM model is to obtain a significant model [27].

To test the significance of the individual model coefficients, the model can be optimized by adding or deleting coefficients through backward elimination, forward addition or stepwise elimination/addition/exchange [28].

The regression equation reveals the relationship between each of the parameters using the experimental data which in turn can be used to estimate the expected values of the response. In this work, the responses chosen are surface roughness, cutting force tool wear and material removal rate.

Design Expert software aids to understand and evaluate the effects of parameters and their interaction effects on the response. It is an efficient tool to optimize processes with one or more responses. Speed (N), feed rate (f), depth of cut (d), the weight percentage of silicon carbide content (w) are chosen as the input parameters. The response surface of various responses can be expressed in terms of these factors as in Eq. (3).

$$\text{Response } Y = f(N, f, d, w) \tag{3}$$

Prediction models for the responses are obtained by nonlinear quadratic backward reduction regression modelling with an exit alpha value of 0.1. The quadratic equations in terms of coded factors for the various objectives are given in Eqs. 4, 5, 6 and 7.

$$Ra = 0.56 + 0.036N + 0.038f + 0.023d + 0.026w \\ - 0.075Nw - 0.027w^2 \tag{4}$$

$$MRR = 2238.93 + 351.69N + 427.2f + 247.23d \\ - 231.44w - 525.25N^2 - 344.03f^2 \\ + 596.37d^2 - 585.52w^2 \tag{5}$$

$$CF = 108.47 + 11.51N - 12.63f + 27.04d - 7.93w \\ - 24.77Nf - 9.75Nw + 12.09fd - 11.94fw \\ + 14.50dw - 7.74N^2 - 16.17w^2 \tag{6}$$

$$TW = 0.25 + 0.090N + 0.031f + 0.028d + 0.055w \\ + 0.014fw + 0.013d^2 + 0.013w^2 \tag{7}$$

3.2 Analysis of variance

The mathematical models obtained are tested for their adequacy through analysis of variance. A greater F value and a lesser p value make the parameters more significant at 95% confidence interval. Tables 3, 4, 5 and 6 show the ANOVA table results from a reduced quadratic model for responses by considering the backward reduction procedure with 0.1 alpha exit value to automatically reduce insignificant terms. Daniel et al. [29] demonstrated in multi-objective optimization of wire electric discharge machining work using the backward reduction procedure of RSM.

Table 2 Experimental results

Run	Spindle speed (N)	Feed rate (f)	Depth of cut (d)	SiC (w)	Ra (μm)	MRR (mm^3/min)	F_z (N)	T_w (mm)
1	+1	0	− 1	0	0.5023	956.3	101.41	0.347
2	0	− 1	+1	0	0.542	1043.48	161.5	0.247
3	0	0	0	0	0.563	2148.95	106.29	0.249
4	0	0	0	0	0.561	2147.93	106.27	0.245
5	− 1	+1	0	0	0.575	925.98	109.31	0.199
6	0	+1	+1	0	0.654	2790.7	107.67	0.298
7	0	+1	0	+1	0.638	1125.98	76.54	0.351
8	0	− 1	− 1	0	0.5342	734.125	80.11	0.2016
9	0	− 1	0	− 1	0.42	805.97	94.48	0.188
10	− 1	0	+1	0	0.5012	812.61	109.5	0.188
11	+1	− 1	0	0	0.587	1303.57	146.58	0.316
12	0	+1	0	− 1	0.521	2109.38	96.36	0.233
13	+1	0	0	+1	0.502	1258.8	59.87	0.401
14	0	0	− 1	− 1	0.523	756.303	89.04	0.184
15	+1	+1	0	0	0.654	2160.00	72.94	0.359
16	0	+1	− 1	0	0.586	1406.25	74.62	0.266
17	0	0	+1	+1	0.5996	812.61	122.56	0.395
18	0	0	0	0	0.562	2148.94	106.29	0.249
19	0	0	+1	− 1	0.534	1506.28	112.34	0.25
20	− 1	0	− 1	0	0.501	759.494	50.75	0.135
21	+1	0	+1	0	0.61	1463.42	148.07	0.379
22	− 1	0	0	+1	0.5623	834.45	68.08	0.231
23	− 1	− 1	0	0	0.521	698.817	83.86	0.136
24	0	− 1	0	+1	0.562	805.97	122.44	0.249
25	0	0	− 1	+1	0.514	762.712	41.24	0.289
26	− 1	0	0	− 1	0.412	1088.71	81.44	0.116
27	+1	0	0	− 1	0.6052	2111.11	112.24	0.288

Table 3 ANOVA table for response surface-reduced quadratic model of surface roughness

Source	Sum of squares	df	Mean square	F value	p value	
Model	0.076	6	0.013	10.69	< 0.0001	Significant
A—Spindle speed	0.016	1	0.016	13.35	0.0016	
B—Feed rate	0.018	1	0.018	15.06	0.0009	
C—Depth of cut	6.55E−03	1	6.55E−03	5.55	0.0288	
D—Percentage of SiC	8.32E−03	1	8.32E−03	7.05	0.0152	
AD	0.023	1	0.023	19.1	0.0003	
D^2	4.81E−03	1	4.81E−03	4.07	0.0572	
Residual	0.024	20	1.18E−03			
Lack of fit	0.024	18	1.31E−03	3934.45	0.0003	Significant
Pure error	6.67E−07	2	3.33E−07			
Cor total	0.099	26				

Table 3 shows the ANOVA table for response surface-reduced quadratic model of surface roughness (Ra). The model F value of 10.69 implies the model is significant. There is only a 0.01% chance that a "model F value" this large could occur due to noise. p value less than 0.05 indicates model terms are significant. In this case A, B, C, D, AD are significant model terms. Values greater than 0.1 indicate the model terms are not significant. The "lack of

Table 4 ANOVA table for response surface-reduced quadratic model of material removal rate

Source	Sum of squares	DF	Mean square	F value	p value	
Model	8.18E+06	8	1.02E+06	9.53	< 0.0001	Significant
A—Spindle speed	1.48E+06	1	1.48E+06	13.83	0.0016	
B—Feed rate	2.19E+06	1	2.19E+06	20.4	0.0003	
C—Depth of cut	7.34E+05	1	7.34E+05	6.83	0.0176	
D—Percentage of SiC	6.43E+05	1	6.43E+05	5.99	0.0249	
A^2	1.47E+06	1	1.47E+06	13.71	0.0016	
B^2	6.31E+05	1	6.31E+05	5.88	0.0261	
C^2	1.90E+06	1	1.90E+06	17.67	0.0005	
D^2	1.83E+06	1	1.83E+06	17.03	0.0006	
Residual	1.93E+06	18	1.07E+05			
Lack of fit	1.88E+06	16	1.18E+05	4.84	0.1844	Not significant
Pure error	48605.4	2	24302.7			
Cor total	1.01E+07	26				

Table 5 ANOVA table for response surface-reduced quadratic model of cutting force

Source	Sum of squares	DF	Mean square	F value	p value	
Model	19672.89	11	1788.44	15.48	< 0.0001	Significant
A—Spindle speed	1590.91	1	1590.91	13.77	0.0021	
B—Feed rate	1913.45	1	1913.45	16.56	0.001	
C—Depth of cut	8773.4	1	8773.4	75.95	< 0.0001	
D—Percentage of SiC	754.78	1	754.78	6.53	0.0219	
AB	2454.71	1	2454.71	21.25	0.0003	
AD	380.45	1	380.45	3.29	0.0896	
BC	584.19	1	584.19	5.06	0.04	
BD	570.73	1	570.73	4.94	0.042	
CD	841.58	1	841.58	7.29	0.0165	
A^2	383.57	1	383.57	3.32	0.0884	
D^2	1673.23	1	1673.23	14.48	0.0017	
Residual	1732.73	15	115.52			
Lack of fit	1732.73	13	133.29	1.48E+05	< 0.0001	Significant
Pure error	1.80E−03	2	9.00E−04			
Cor total	21405.61	26				

Table 6 ANOVA table for response surface-reduced quadratic model of Tool wear

Source	Sum of squares	df	Mean square	F value	p value	
Model	0.16	7	0.022	102.64	< 0.0001	Significant
A—Spindle speed	0.098	1	0.098	447.86	< 0.0001	
B—Feed rate	0.011	1	0.011	51.63	< 0.0001	
C—Depth of cut	9.32E−03	1	9.32E−03	42.54	< 0.0001	
D—Percentage of SiC	0.036	1	0.036	164.22	< 0.0001	
BD	8.12E−04	1	8.12E−04	3.71	0.0692	
C^2	1.16E−03	1	1.16E−03	5.31	0.0327	
D^2	1.07E−03	1	1.07E−03	4.87	0.0399	
Residual	4.16E−03	19	2.19E−04			
Lack of fit	4.16E−03	17	2.45E−04	244.7	0.0041	Significant
Pure error	2.00E−06	2	1.00E−06			
Cor total	0.16	26				

fit F value" of 3934.45 implies the lack of fit is significantly relative. There is only a 0.03% chance that a "lack of fit F value" this large could occur due to noise. R-squared value is 0.7624. The "Pred R-squared" of 0.5167 is in reasonable agreement with the "Adj R-squared" of 0.6911.

Table 4 indicates the analysis of variance for response surface-reduced quadratic model of MRR. The model F value of 9.53 implies the model is significant. There is only a 0.01% chance that a "model F value" this large could occur due to noise. Values of "Prob > F" less than 0.05 indicate model terms are significant. In this case A, B, C, D, A^2, B^2, C^2, D^2 are significant model terms. Values greater than 0.1 indicate the model terms are not significant. The "lack of fit F value" of 4.84 implies the lack of fit is not significantly relative to the pure error. There is a 18.44% chance that a "lack of fit F value" this large could occur due to noise. R-squared value is 0.8090. R-squared value is 0.9191. The "Pred R-squared" of 0.5702 is in reasonable agreement with the "Adj R-squared" of 0.7241.

Table 5 reveals about the variance of analysis of reduced quadratic model for cutting force. The model F value of 15.48 implies the model is significant. There is only a 0.01% chance that a "model F value" this large could occur due to noise. In this case A, B, C, D, AB, BC, BD, CD, D^2 are significant model terms. Here is only a 0.01% chance that a "lack of fit F value" this large could occur due to noise. The "Pred R-squared" of 0.6872 is in reasonable agreement with the "Adj R-squared" of 0.8597.

Table 6 depicts the information of ANOVA for response surface-reduced quadratic model of tool wear. The model F value of 102.64 implies the model is significant. There is only a 0.01% chance that a "model F value" this large could occur due to noise. In this case A, B, C, D, C^2, D^2 are significant model terms. There is only a 0.41% chance that a "lack of fit F value" this large could occur due to noise. R-squared value is 0.9742. The "Pred R-squared" of 0.9391 is in reasonable agreement with the "Adj R-squared" of 0.9647.

Tables 7, 8, 9 and 10 show the confidence interval results of standard error for the responses of surface roughness, MRR, cutting force and tool wear.

Normal probability plot of residual is a diagnostic checking tool for normality of residuals of developed response surface model. From Fig. 5a–d, it is observed that distributed residuals are almost proportional to the normal probability following a straight line pattern, indicating that the errors are distributed normally.

3.3 Effect of SiC on machinability

Machinability means good performance regarding surface finish, cutting power consumption, material remove rate, chip removal and tool life, surface finish. Lui et al. [30] studied on the interaction of the cutting tools and the ceramic-reinforced metal matrix composites during micro-machining. In particulate MMCs, the effects of particle shapes (aspect ratio), particle size and volume fraction have a substantial influence on the micro-cutting performance. Hence, the effect of the weight percentage of the reinforcement (SiC) with the most influencing parameter on the machinability characteristics was studied.

Figure 6 represents the surface plot of surface roughness with respect to varying spindle speed and weight percentage of SiC. The figure shows that surface roughness increases with increase in spindle speed.

From Fig. 6, it can be observed that the surface roughness increased by increasing the percentage of SiC at the hold value of feed rate of 0.03 mm/rev. Likewise, increasing the spindle speed from 1000 to 2000 rpm, the surface roughness increased at 5 wt% of SiC. The combination of lower percentage of SiC and higher spindle speed exhibited the higher surface roughness. The cutting speed plays the major role in deciding the surface roughness. Generally, at higher speeds minimum surface roughness is achieved, and at lower speeds, the surface is rougher due to the formation of built-up edges (BUE). But in this composite, due to the presence of reinforcements and higher tool wear at increased speeds, increasing side flow of aluminium metal which outweighs the effect of reduced cutting forces, surface roughness increases at increased speeds.

From Fig. 7, it can be examined that MRR increases gradually by increasing the addition of SiC from 5 to

Table 7 Confidence interval for surface roughness

Factor	Coefficient estimate	df	Standard error	95% CI low	95% CI high	VIF
Intercept	0.56	1	8.87E−03	0.55	0.58	
A—Spindle speed	0.036	1	9.92E−03	0.016	0.057	1
B—Feed rate	0.038	1	9.92E−03	0.018	0.059	1
C—Depth of cut	0.023	1	9.92E−03	2.67E−03	0.044	1
D—Percentage of SiC	0.026	1	9.92E−03	5.64E−03	0.047	1
AD	− 0.075	1	0.017	− 0.11	− 0.039	1
D^2	− 0.027	1	0.013	− 0.055	9.01E−04	1

Table 8 Confidence interval for MRR

Factor	Coefficient estimate	df	Standard error	95% CI low	95% CI high
Intercept	2238.93	1	189.16	1841.53	2636.3
A—Spindle speed	351.69	1	94.58	152.99	550.4
B—Feed rate	427.2	1	94.58	228.49	625.9
C—Depth of cut	247.23	1	94.58	48.53	445.93
D—Percentage of SiC	− 231.44	1	94.58	− 430.14	− 32.73
A^2	− 525.25	1	141.87	− 823.3	− 227.2
B^2	− 344.03	1	141.87	− 642.08	− 45.98
C^2	− 596.37	1	141.87	− 894.43	− 298.32
D^2	− 585.52	1	141.87	− 883.58	− 287.47

Table 9 Confidence interval for cutting force

Factor	Coefficient estimate	df	Standard error	95% CI low	95% CI high	VIF
Intercept	108.47	1	3.58	100.83	116.11	1
A—Spindle speed	11.51	1	3.1	4.9	18.13	1
B—Feed rate	− 12.63	1	3.1	− 19.24	− 6.01	1
C—Depth of cut	27.04	1	3.1	20.43	33.65	1
D—Percentage of SiC	− 7.93	1	3.1	− 14.54	− 1.32	1
AB	− 24.77	1	5.37	− 36.23	− 13.32	1
AD	− 9.75	1	5.37	− 21.21	1.7	1
BC	− 12.09	1	5.37	− 23.54	− 0.63	1
BD	− 11.94	1	5.37	− 23.4	− 0.49	1
CD	14.5	1	5.37	3.05	25.96	1.04
A^2	− 7.74	1	4.25	− 16.8	1.31	1.04
D^2	− 16.17	1	4.25	− 25.22	− 7.11	1

Table 10 Confidence interval for tool wear

Factor	Coefficient estimate	df	Standard error	95% CI low	95% CI high	VIF
Intercept	0.25	1	4.93E−03	0.24	0.26	
A—Spindle speed	0.09	1	4.27E−03	0.081	0.099	1
B—Feed rate	0.031	1	4.27E−03	0.022	0.04	1
C—Depth of cut	0.028	1	4.27E−03	0.019	0.037	1
D—Percentage of SiC	0.055	1	4.27E−03	0.046	0.064	1
BD	0.014	1	7.40E−03	− 1.24E−03	0.03	1
C^2	0.013	1	5.85E−03	1.24E−03	0.026	1.04
D^2	0.013	1	5.85E−03	6.62E−04	0.025	1.04

10 wt% at a spindle speed rate of 1000 rpm. Further increase in SiC causes decrease in MRR. It is clear from the plot that the combination of lower percentage of SiC and higher spindle speed causes higher amount of material removal. As SiC content increases, the brittleness of the composite increases leading to the disappearance of BUE. Increased reinforcements hindered material removal rate due to their increased hardness

From Fig. 8, it has been examined that cutting force increases with increase in spindle speed. When the spindle speed is fixed at 1000 rpm and increasing the percentage of SiC from 5% to 15%, cutting force increases up to a certain

limit of 10 wt% of SiC reinforcement and then cutting force decreases. The formation of the built-up edge (BUE) on the tools and change in the thickness of the chips removed from the workpiece material is very important in determining cutting force values. Though increased reinforcements result in the disappearance of BUE, accelerated tool wear at a high volume fraction of SiC increases the cutting force required to cut the material (Fig. 8). Also cutting force modelling has to be done on a microscale as the tool encounters the harder reinforcements and matrix alternatively.
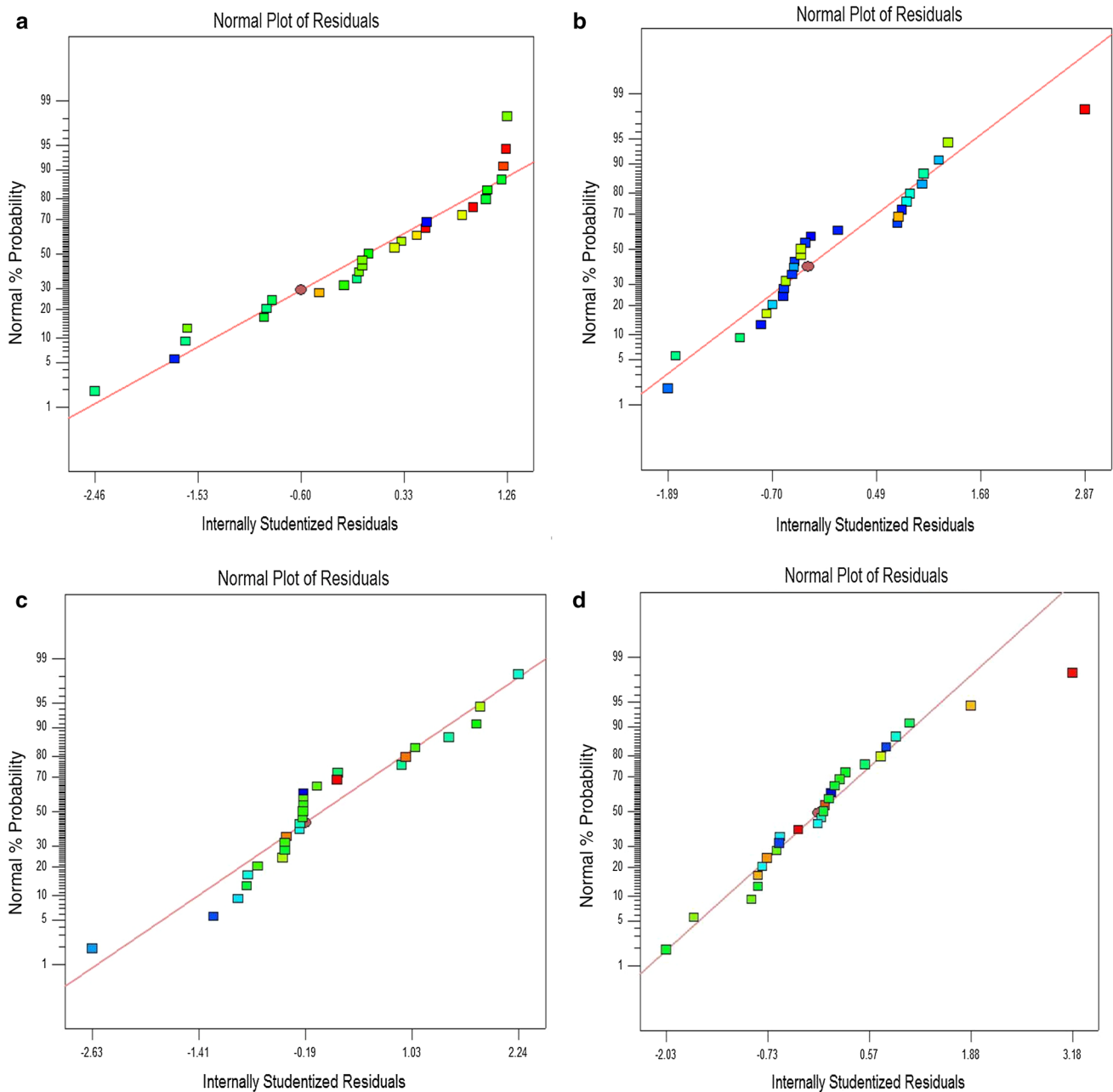
Fig. 5 Normal probability plots of residuals for **a** surface roughness, **b** material removal rate, **c** cutting force, **d** tool wear

The response plot for tool wear (Fig. 9) shows a linear curve. As the percentage of SiC and spindle speed increase, tool wear also increased. At a lower spindle speed, tool wear is less, and the formation of unstable larger BUE at a low spindle speed protects the cutting edge from further wear. But with an increase in spindle speed, an increase in tool wear is observed, due to the formation of high temperature at high spindle speed and thermal softening at cutting edge. The results were similar to the work concluded by the researcher Ozben et al. [31].

3.4 Multi-objective optimization solutions using RSM

A set of multi-response optimization solution for minimum surface roughness, cutting force, tool wear and maximum material removal rate is given in Table 11. The optimum point of prediction of multi-response characteristics of fine surface finish, least cutting force, tool wear and maximum MRR is shown in Table 12. The purpose of the confirmation test is to validate the results drawn during the tests. Once the optimum level of the process parameters is
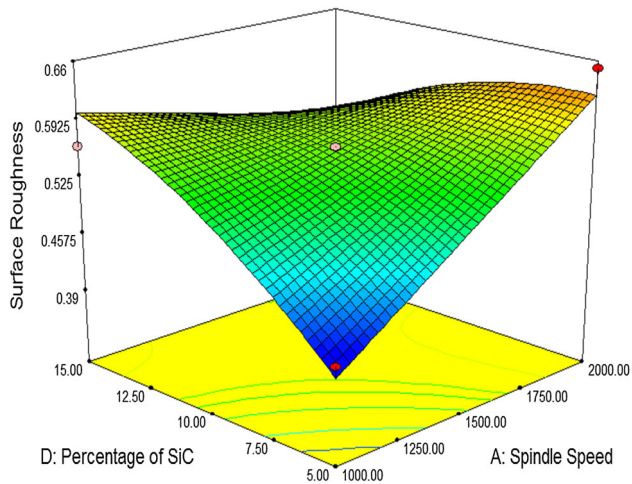
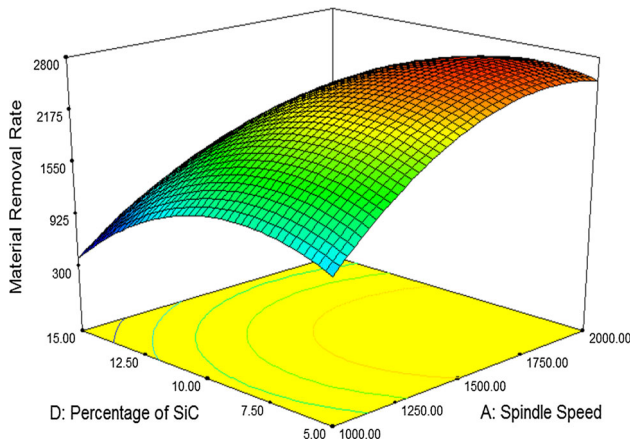Fig. 6 Surface plot of Surface roughness
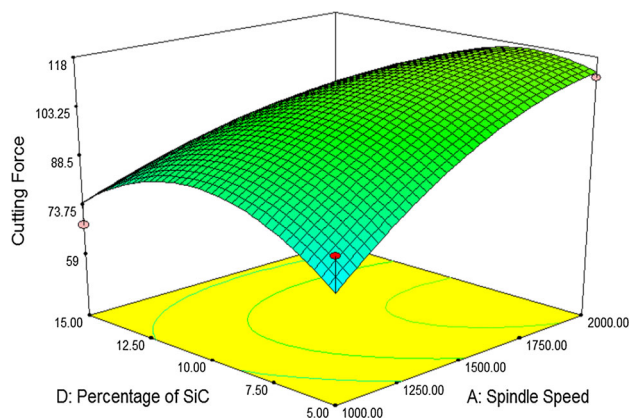

Fig. 7 Surface plot of MRR

Fig. 8 Surface plot of cutting force

selected, the last step is to predict and verify the improvement of the machinability characteristics using the optimum level of the parameters.

Confirmatory tests were conducted twice with the settings of solution 9. The confirmatory test results show the
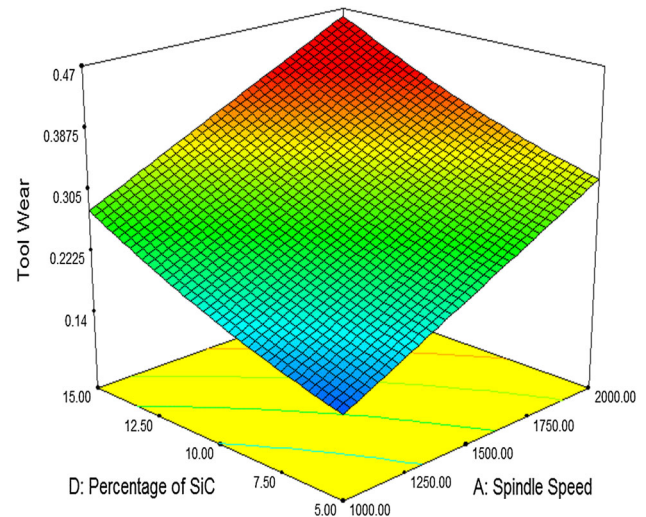

Fig. 9 Surface plot of tool wear

values of Ra as 0.49 μm and 0.47 μm, MRR as 1745 mm^3/min and 1689 mm^3/min, Fz as 96.2 N and 101.7 N and, T_w as 0.23 mm and 0.15 mm for the two runs. Table 13 shows confirmatory result with 95% confidence level. Confirmation is intended to be used to confirm that the model can predict actual outcomes at the optimal settings determined from the analysis. Two ($n = 2$) runs are conducted at the optimal settings. The average of those runs is compared to the prediction interval for a sample of size n. The larger the n, the smaller the interval. Smaller intervals indicate good precision in the estimates. If the sample size is one, then it can be thought of as the next observation. A prediction interval will be larger (a wider spread) than the confidence interval because there is more scatter expected from a small sample estimating the average versus the entire population's true mean.

Multi-response optimization by RSM shows that the minimum value of surface roughness during end milling aluminium composites can be obtained at spindle speed of 1210 rpm, feed rate of 0.033 mm/rev, depth of cut of 1.6 mm and 5% of SiC.

3.5 Optimization using multi-objective genetic algorithm

The aim of this work is to simultaneously optimize surface roughness, material removal rate, cutting force and tool wear as to (1) minimize surface roughness (Ra), (2) maximize material removal rate (MRR), (3) minimize cutting force (F_z) and (4) minimize tool wear (T_w).

Genetic algorithm is a popularly used meta-heuristic tool for multi-objective optimization. Multi-objective GA generates a set of Pareto-optimal solutions which are each good in some respect. Optimization is done using multi-

Table 11 Multi-response solutions

S. No.	Spindle speed	Feed rate	Depth of cut	Percentage of SiC	Ra (μm)	MRR (mm³/min)	F_z (N)	T_w (mm)
1	1208	0.032	1.600	5.000	0.451	1596	89.891	0.163
2	1206	0.032	1.597	5.000	0.451	1593	89.777	0.162
3	1207	0.032	1.598	5.000	0.452	1589	89.685	0.162
4	1208	0.032	1.605	5.000	0.451	1601	90.089	0.163
5	1209	0.033	1.598	5.000	0.452	1602	90.013	0.163
6	1203	0.032	1.608	5.000	0.451	1591	89.935	0.162
7	1209	0.032	1.608	5.000	0.451	1601	90.089	0.163
8	1205	0.033	1.605	5.000	0.451	1601	90.135	0.163
9	1210	0.033	1.605	5.000	0.450	1611	90.303	0.164

Table 12 Optimum point of prediction

Solution 1 of 9 response	Predicted mean	Predicted median	SD	SE mean	95% CI low for mean	95% CI high for mean	95% TI low for 99% pop	95% TI high for 99% pop
Surface roughness	0.460	0.460	0.0343565	0.018276	0.422128	0.498376	0.308584	0.611919
Material removal rate	1605.33	1605.33	296.766	177.151	1219.35	1991.31	131.26	3079.41
Cutting force	90.3411	90.3411	10.7478	6.02053	77.5086	103.174	39.9957	140.686
Tool wear	0.16122	0.16122	0.0148002	0.007246	0.146053	0.176387	0.0964461	0.225994

Table 13 Experimental and predicted values of results—two-sided, confidence = 95%

Solution 9 of response	Predicted mean	Predicted median	SD	n	SE Pred	95% PI low	Data mean	95% PI HIGH
Surface roughness	0.462	0.462	0.0343	2	0.02994	0.3999	0.4	0.5248
Material removal rate	1611	1611	296.76	2	270.846	1021.8	1717	2202
Cutting force	90.64	90.64	10.747	2	9.50771	70.376	98.95	110
Tool wear	0.16	0.16	0.0148	2	0.01252	0.1344	0.19	0.1868

objective genetic algorithm and direct search tool box. Because of the conflicting nature of performance measures, a single combination of input parameters does not serve the purpose. As a result, a set of optimal solutions (i.e., Pareto-optimal solutions) is achieved instead of a single solution. Pareto-front plots the function values for all non-inferiority solutions of Ra and MRR as shown in Fig. 10.

The non-dominated Pareto-optimal solutions are listed in Table 14. These points can be plotted between any two objective functions to form the Pareto-front. Figure 10 shows the Pareto-front drawn between surface roughness and material removal rate. Points 1–4 show a very good surface finish but at the cost of material removal rate. Though the roughness values fall within 0.3 microns, the material removal is less than 1100 mm³/min. Points 6–10

show a moderate surface finish with a good increase in material removal rate (1000–2050 mm³/min). Points 12–14 pertain to a very high material removal of more than 2000 mm³/min with surface roughness values falling between 0.8 and 1.20 microns.

Studying Table 14, several decisions may be made, depending on the real conditions. For instance, the most suitable machining parameters should match the solution 14 when the power consumption is an important concern since cutting force is a direct predictor of power consumption. But at these cutting conditions, material removal is not so appreciable which means that the production time increases. The choice of solution will essentially depend on the working environment. Similar observations were made in the research of Pushpendra et al. [32].
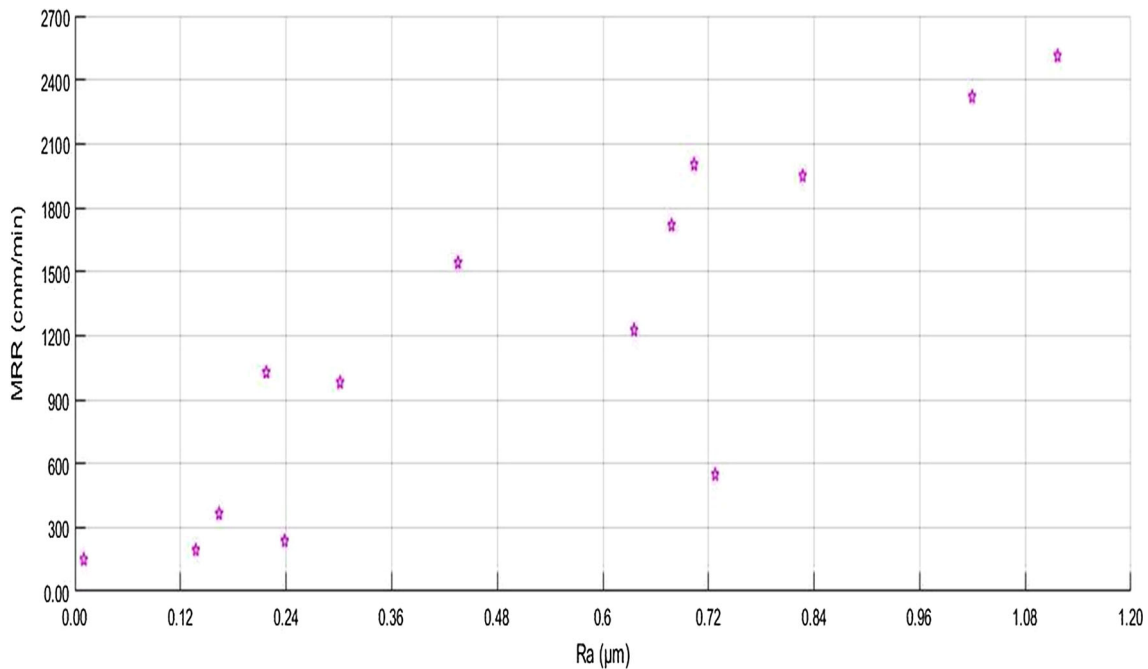
Fig. 10 Pareto-front—Ra and MRR

Table 14 Pareto-optimal solutions

Points	Spindle speed (rpm)	Feed rate (mm/rev)	DoC (mm)	SiC (%)	Ra (µm)	MRR (mm³/min)	F_z (N)	T_w (mm)
1	1032	0.03	1.07	5	0.02	152	50.3	0.106
2	1300	0.02	1.07	5	0.14	213	68.1	0.15
3	1386	0.04	1.07	15	0.17	327	11.7	0.421
4	1459	0.04	1.12	15	0.22	1043	22.9	0.412
5	1548	0.03	1.38	6	0.237	282	116.1	0.240
6	1511	0.03	1.27	6	0.31	1021	122.9	0.349
7	1885	0.04	1.17	13	0.44	1506	61.8	0.397
8	1924	0.04	1.28	12	0.64	1202	59.5	0.372
9	1764	0.03	1.85	7	0.69	1724	124.9	0.288
10	1958	0.04	1.65	15	0.71	2034	44.7	0.443
11	1934	0.04	1.76	12	0.728	586	78.7	0.390
12	1881	0.04	1.84	6	0.83	1967	96.1	0.356
13	1957	0.04	1.87	13	1.02	2356	131.2	0.487
14	1953	0.04	1.8	7	1.09	2513	93.3	0.367

3.6 Confirmatory runs

The multi-responses were tested after the MOGA modelling to identify the input parameters settings that would meet the requirement. Confirmatory runs were conducted at these required settings of Pareto-optimal solution points 6 and 13 (moderate surface roughness and maximum material rate) for a speed of 1511 and 1957 rpm. The experimental values were found to be in close agreement with the predictions. The values are tabulated in Table 15.

The workpiece prepared at the confirmatory test settings was machined at two depths of cut (1.27 mm and 1.87 mm), and their chip forms were observed. It was seen that these chips were easily freeable and they do not coil up continuously as while machining aluminium. It is also observed that chips formed were not of the same form in composites with a non-uniform distribution. The chips

Table 15 Experimental and predicted values of results

S. No	N (rpm)	f (mm/rev)	d (mm)	w (%)	Ra (μm)		MRR (mm^3/min)		F_z (N)		T_w (mm)	
					Pred	Exp	Pred	Exp	Pred	Exp	Pred	Exp
1	1511	0.03	1.27	6	0.31	0.36	1021	1037	122.9	116.8	0.35	0.38
2	1957	0.04	1.87	13	1.02	1.05	2356	2349	91.2	131.2	0.49	0.50

produced at 1.27 and 1.87 mm depth of cut are shown in Fig. 11a, b.

It is observed that these chips were almost discontinuous and unlike those obtained while machining aluminium. These chips easily got broken from the surface of the workpiece and tool without hindering machining. In composites with inhomogeneous distribution, continuous chips were formed in one part of the composite and high heat generation was observed at the other area which may be attributed to the presence of unreinforced matrix areas and particle agglomeration in the other area.

4 Conclusion

Composites are novel materials which provide a new approach for material engineers to design the material and its properties based on their functional requirement with proper compositions of matrix and reinforcements. With a view of designing the composite for improved machinability, this paper aims to simultaneously optimize several responses which are a measure of machinability under a set of practical machining constraints. The combined effect of alumina and SiC has been studied to optimize the weight percentage of reinforcements.

Multi-response optimization by RSM shows that the minimum value of surface roughness (0.46 μm), cutting force (90.3411 N), tool wear (0.161 mm), maximum material removal rate (1605.33 mm^3/min) during end milling AA7075 hybrid composite can be achieved at

spindle speed of 1210 rpm, feed rate of 0.033 mm/rev, depth of cut of 1.6 mm and 5% of SiC.

Pareto-optimal solutions can be used to find the multiple sets of optimal solutions so as to empower a manufacturing engineer to determine an appropriate optimal accomplishing set of input variables according to the specific engineering requirement. Confirmatory test was conducted for two of the Genetic algorithm predicted Pareto-optimal settings and the test results go closely with the predicted values. The explicit process models connecting the controllable process parameters with output variables such as cutting force, material removal, tool wear and generated surface roughness for advanced varied materials during end milling process will reasonably improve the industrial needs of MMCs processing.

References

1. Muthukrishnan N, Paulo Davim J (2009) Optimization of machining parameters of Al/SiC-MMC with ANOVA and ANN analysis. J Mater Process Technol 209:225–232. https://doi.org/10.1016/j.jmatprotec.2008.01.041

2. Altunpak Y, Ay M, Aslan S (2012) Drilling of a hybrid Al/SiC/Gr metal matrix composites. Int J Adv Manuf Technol 60(5–8):513–517. https://doi.org/10.1007/s00170-011-3644-4

3. Bhushan RK (2013) Optimization of cutting parameters for minimizing power consumption and maximizing tool life during machining of Al alloy SiC particle composites. J Clean Prod 39:242–254. https://doi.org/10.1016/j.jclepro.2012.08.008

4. Arun Premnath A, Alwarsamy T, Abhinav T, Adithya Krishnakant C (2012) Surface roughness prediction by response surface methodology in milling of hybrid aluminium composites. Procedia Eng 38:745–752. https://doi.org/10.1016/j.proeng.2012.06.094

5. Dikshit MK, Puri AB, Maity A (2014) Experimental study of cutting forces in ball end milling of Al2014-T6 using response surface methodology. Procedia Mater Sci 6:612–622. https://doi.org/10.1016/j.mspro.2014.07.076

6. Lebaal N, Nouari M, Ginting A (2011) A new optimization approach based on Kriging interpolation and sequential quadratic programming algorithm for end milling refractory titanium alloys. Appl Soft Comput 11:5110–5119. https://doi.org/10.1016/j.asoc.2011.05.048
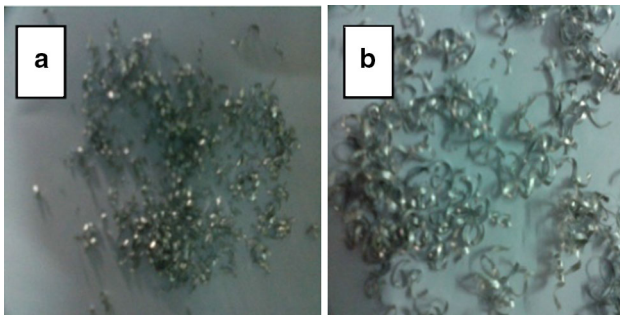

Fig. 11 Chip form of confirmatory test machined samples. **a** Speed 1511 rpm, feed 0.03 mm/rev., **b** speed 1957 rpm, feed 0.04 mm/rev

7. Arokiadass R, Palaniradja K, Alagumoorthi N (2012) Prediction and optimization of end milling process parameters of cast aluminium based MMC. Trans Nonferrous Met Soc China 22:1568–1574. https://doi.org/10.1016/S1003-6326(11)61357-5

8. Sreenivasulu R (2013) Optimization of surface roughness and delamination damage of GFRP composite material in end milling using Taguchi design method and artificial neural network. Procedia Eng 64:785–794. https://doi.org/10.1016/j.proeng.2013.09.154

9. Li W, Guo YB, Barkey ME, Jordon JB (2014) Effect tool wear during end milling on the surface integrity and fatigue life of inconel 718. Procedia CIRP 14:546–551. https://doi.org/10.1016/j.procir.2014.03.056

10. Zain AM, Haron H, Sharif S (2010) Prediction of surface roughness in the end milling machining using artificial neural network. Expert Syst Appl 37:1755–1768. https://doi.org/10.1016/j.eswa.2009.07.033

11. Yan J, Li L (2013) Multi-objective optimization of milling parameters—the trade-offs between energy, production rate and cutting quality. J Clean Prod 52:462–471. https://doi.org/10.1016/j.jclepro.2013.02.030

12. Yusup N, Zain AM, Hashim SZM (2012) Evolutionary techniques in optimizing machining parameters—review and recent applications (2007–2011). Expert Syst Appl 39:9909–9927. https://doi.org/10.1016/j.eswa.2012.02.109

13. Mukherjee I, Ray PK (2006) A review of optimization techniques in metal cutting processes. Comput Ind Eng 50:15–34. https://doi.org/10.1016/j.cie.2005.10.001

14. Jawahir IS, Brinksmeier E, M'Saoubi R, Aspinwall DK, Outeiro JC, Meyer D, Umbrello D, Jayal AD (2011) Surface integrity in material removal processes: recent advances. CIRP ANN Manuf Technol 60:603–626. https://doi.org/10.1016/j.cirp.2011.05.002

15. D'Addona DM, Teti R (2013) Genetic algorithm-based optimization of cutting parameters in turning processes. Procedia CIRP 7:323–328. https://doi.org/10.1016/j.procir.2013.05.055

16. Senthilkumar C, Ganesan G, Karthikeyan R (2010) Bi-performance optimization of electrochemical machining characteristics of Al/20%SiCp composites using NSGA-II. Proc Inst Mech E Part B J Eng Manuf 224:1399–1407. https://doi.org/10.1243/09544054JEM1803

17. Vijay Kumar K, Naveen Sait A, Panneerselvam K (2014) Machinability study of hybrid-polymer composite pipe using response surface methodology and genetic algorithm. J Sandw Struct Mater 16(4):418–439. https://doi.org/10.1177/1099636214532115

18. Majumder A (2014) Comparative study of three evolutionary algorithms coupled with neural network model for optimization of electric discharge machining process parameters. Proc Inst Mech Eng Part B J Eng Manuf. https://doi.org/10.1177/0954405414538960

19. Shahali H, Yazdi MRS, Mohammad A, Iimanian E (2012) Optimization of surface roughness and thickness of white layer in wire electrical discharge machining of DIN 1.4542 stainless steel using micro-genetic algorithm and signal to noise ratio techniques. Proc Inst Mech Eng E Part B J Eng Manuf 226(5):803–812. https://doi.org/10.1177/0954405411434234

20. Thangarasu VS, Devaraj G, Sivasubramanian R (2012) High speed CNC machining of AISI 304 stainless steel; Optimization of process parameters by MOGA. Int J Eng Sci Technol 4(3):66–77

21. Ganesan H, Mohankumar G (2013) Optimization of machining techniques in CNC turning centre using genetic algorithm. Arab J Sci Eng 38:1529–1538. https://doi.org/10.1007/s13369-013-0539-8

22. Mahfouf M, Jamei M, Linkens DA (2005) Optimal design of alloy steels using multiobjective genetic algorithms. Mater Manuf Process 20:553–567. https://doi.org/10.1081/AMP-200053580

23. Yadav RN, Yadava V, Singh GK (2014) Application of non-dominated sorting genetic algorithm for multi-objective optimization of electrical discharge diamond face grinding process. J Mech Sci Technol 28(6):2299–2306. https://doi.org/10.1007/s12206-014-0520-9

24. Santhanakrishnan M, Sivasakthivel PS, Sudhakaran R (2015) Modeling of geometrical and machining parameters on temperature rise while machining Al 6351 using response surface methodology and genetic algorithm. J Braz Soc Mech Sci Eng 39(2):487–496. https://doi.org/10.1007/s40430-015-0378-5

25. Malghan RL, Rao KMC, Shettigar AK, Rao SS, D'Souza RJ (2017) Application of particle swarm optimization and response surface methodology for machining parameters optimization of aluminium matrix composites in milling operation. J Braz Soc Mech Sci Eng 39(9):3541–3553. https://doi.org/10.1007/s40430-016-0675-7

26. Prabhu S, Uma M, Vinayagam BK (2014) Electrical discharge machining parameters optimization using response surface methodology and fuzzy logic modeling. J Braz Soc Mech Sci Eng 36:637–652. https://doi.org/10.1007/s40430-013-0112-0

27. Montgomery DC (2009) Design and analysis of experiments, 7th edn. Wiley, Singapore, pp 207–264

28. Noordin MY, Venkatesh VC, Sharif S, Elting S, Abdullah A (2004) Application of response surface methodology in describing the performance of coated carbide tools when turning AISI 1045 steel. J Mater Process Technol 145:46–58

29. Ghodsiyeh D, Golshan A, Izman S (2014) Multi-objective process optimization of wire electrical discharge machining based on response surface methodology. J Braz Soc Mech Sci Eng 36(2):310–313. https://doi.org/10.1007/s40430-013-0079-x

30. Liu J, Li J, Xu C (2014) Interaction of the cutting tools and the ceramic-reinforced metal matrix composites during micro-machining: a review. CIRP J Manuf 7(2):55–70. https://doi.org/10.1016/j.cirpj.2014.01.003

31. Ozben T, Kilickap E, Cakır O (2008) Investigation of mechanical and machinability properties of SiC particle reinforced Al-MMC. J Mater Process Technol 198:220–225. https://doi.org/10.1016/j.jmatprotec.2007.06.082

32. Pushpendra Bharti S, Maheshwari S, Sharma C (2012) Multi-objective optimization of electric-discharge machining process using controlled elitist NSGA-II. J Mech Sci Technol 26(6):1875–1883. https://doi.org/10.1007/s12206-012-0411-x